Journal of Alloys and Compounds 502 (2010) 215–219

Contents lists available at ScienceDirect

Journal of Alloys and Compounds

journal homepage: www.elsevier.com/locate/jallcom

The influence of holding time on the performance of $LiNi_{0.5}Mn_{1.5}O_4$ cathode for lithium ion battery

Tongyong Yang[a], Kening Sun[b,*], Zhengyu Lei[a], Naiqing Zhang[b,*], Ye Lang[a]

[a] Department of Chemistry, Harbin Institute of Technology, Harbin 150001, PR China
[b] Academy of Fundamental and Interdisciplinary Sciences, Harbin Institute of Technology, Harbin, Heilongjiang 150001, PR China

ARTICLE INFO

Article history:
Received 7 March 2010
Accepted 20 April 2010
Available online 31 May 2010

Keywords:
Lithium nickel manganese oxide
Cathode
Lithium ion battery
High voltage
Holding time

ABSTRACT

The development of heterogeneous $LiNi_{0.5}Mn_{1.5}O_4$ spinel for high power lithium ion battery applications has been investigated during last decades. In this study, $LiNi_{0.5}Mn_{1.5}O_4$ cathode materials are successfully prepared with sol–gel method, and the influence of holding time on performances of the $LiNi_{0.5}Mn_{1.5}O_4$ cathode is investigated. The results show that the holding time has a remarkable effect on the crystallinity, the morphology, the purity, the Mn^{3+} amount, and the grain size distribution, then further impacts the related electrochemical behaviors. We find that a decomposition reaction of the spinel occurs when an overlong holding time is used to synthesize the spinel powder, and the rate performance is directly related with the Mn^{3+} amount. We experimentally suggest that the compound sintered for 18 h exhibits the good electrochemical response in terms of both cycling and rate properties.

1. Introduction

In the past years a considerable attention has been paid to alternative energy sources, in particular to lithium ion batteries owing to their long lifespan and high energy density, with environmental (non-contaminating materials) and other ecological considerations (such as the CO_2/global warming issue, etc.) being of primary importance [1–3]. The requirements from electric vehicles (EV) or hybrid electric vehicles (HEV) in the case of start-up, speedup and grade climbing [4], specially, for zero emission vehicles applications, ask for massive commercial lithium ion batteries. The using of cathodes with potential higher than 4 V (versus Li/Li^+) in lithium ion battery can largely reduce the amount of assembled batteries used for EV. Moreover, cathodes with high voltage can not only allow anodes working significantly above 0 V, then avoiding the formation of metallic Li [5], but also enhance the total output voltage of batteries. The spinel $LiNi_{0.5}Mn_{1.5}O_4$ compound exhibits a high voltage of about 4.7 V in charge/discharge process [6], which is a promising cathode material for lithium ion battery.

The synthesis condition is crucial to obtain the high performance $LiNi_{0.5}Mn_{1.5}O_4$, which is necessary for practical utilization. High temperature calcination is one of must do processes to produce $LiNi_{0.5}Mn_{1.5}O_4$ crystalline. However, the oxygen release from the lattice is a common unavoidable reaction when the sintering temperature is higher than 650 °C as shown in the following reaction [7,8]:

$$LiNi_{0.5}Mn_{1.5}O_4 \rightarrow \alpha Li_xNi_{1-x}O(NiO) + \beta LiMn_{1.5+y}Ni_{0.5-y}O_4 + \gamma O_2 \quad (1)$$

therefore the oxygen release can format the product with a secondary phase of NiO or $Li_xNi_{1-x}O$, thus, developing the 4 V plateau during discharge, decreasing the 5 V capacity and deteriorating the electrochemical behaviors of the material [9]. The appearance of voltage plateaus around 5 V and 4 V regions corresponds to the redox reactions of Ni^{2+}/Ni^{4+} [10] and Mn^{3+}/Mn^{4+} [6]. It is well documented that the properties of $LiNi_{0.5}Mn_{1.5}O_4$, specially the electrochemical behaviors, are depended on synthesis methods, including molten salt method [11], sol–gel method [12,13], solid-state method [14,15], emulsion drying method [16], composite carbonate process [2], and co-precipitation [17]. The wide-used sol–gel method shows advantages in homogeneously mixing the reactors at atomic or molecular level, extremely controlling the stoichiometric amount, easily controlling the producer with uniform particle size [18,19]. High temperature calcination is sequentially executed after homogeneously mixing all raw reagents. Some researchers have synthesized this spinel material with the sol–gel method [20–22]. Recently, Hwang prepared a series of $LiNi_{0.5}Mn_{1.5}O_4$ spinels and pointed out that the performances were strongly depended on the sintering temperature [13]. However, up to our knowledge, the systematic investigation on holding time

* Corresponding authors at: Academy of Fundamental and Interdisciplinary Sciences, Harbin Institute of Technology, P.O. Box 211, No. 92 West Dazhi Street, Harbin, Heilongjiang 150001, PR China. Tel.: +86 451 8641 2153; fax: +86 451 8641 2153.
E-mail addresses: keningsun@yahoo.com.cn (K. Sun), znqmww@163.com (N. Zhang).

0925-8388/$ – see front matter © 2010 Elsevier B.V. All rights reserved.
doi:10.1016/j.jallcom.2010.04.149

which should also have dramatic influence on performances is not documented in the literatures.

In this study, $LiNi_{0.5}Mn_{1.5}O_4$ was prepared with sol–gel method. The results show that the holding time has a significant influence on the morphology, the purity, the Mn^{3+} amount, and the grain size distribution, then further impacts the related electrochemical behaviors.

2. Experimental

2.1. Synthesis procedure

All chemical reagents used in this study were A.R. grade. $LiNi_{0.5}Mn_{1.5}O_4$ powders were prepared with sol–gel method. In brief, $LiOH{\cdot}H_2O$, $Ni(CH_3COO)_2{\cdot}4H_2O$, and $Mn(CH_3COO)_2{\cdot}4H_2O$ (cationic mole ratio of Li:Ni:Mn = 1:0.5:1.5) were firstly dissolved in distilled water and added to a continuously stirred aqueous solution of citric acid. After adjusting the pH of the solution to 7.0 by adding ammonium hydroxide, the solution was evaporated at 75 °C until to obtain a wet gel. Then, the gel was dried at 90 °C under vacuum atmosphere for overnight, and pre-sintered at 450 °C for 5 h in air. Thereafter, the obtained powders were calcined at 850 °C for various holding times. For convenience, the final spinel materials sintered for 6 h, 12 h, 18 h, and 24 h were marked as A, B, C, and D, respectively.

2.2. Characterizations of $LiNi_{0.5}Mn_{1.5}O_4$ powder

The powder X-ray diffraction (XRD) was used to character the crystallographic structure of $LiNi_{0.5}Mn_{1.5}O_4$ powder on Rigaku D/max-2000 X-ray diffractometer with monochromated Cu Ka radiation (45 kV, 50 mA). The Fourier transform infrared spectra (FTIR) of samples were performed on an Avatar 360 FTIR spectrophotometer (NICOLET) using KBr pellet technique. The particle morphology of powders was observed using a scanning electron microscope (SEM, HITACHI, S-4700).

2.3. Electrochemical tests

The as-prepared $LiNi_{0.5}Mn_{1.5}O_4$, carbon black and polyvinylidene fluoride were mixed with a weight ratio of 8:1:1 in N-methyl pyrrolidinone to prepare the positive electrode. The slurry was coated onto an aluminum foil with doctor blade technique, and dried at 120 °C for 12 h in vacuum, then dried again at 80 °C for more than 10 h in vacuum after being pressed. CR2025 button testing cells, using pure metallic lithium disc and $LiNi_{0.5}Mn_{1.5}O_4$ film as anode and cathode, porous polypropylene film as separator, respectively, were assembled in an argon-filled glove box. The electrolyte (1 M $LiPF_6$ in ethylene carbonate and dimethyl carbonate, 1:1 volume rate) was injected in testing batteries. A neware battery testing system (CT-3008W) was used for cycling and rate capability testing in the range from 3.0 V to 4.95 V at special rate (the calculated 1 C = 148 mA g^{-1}) at room temperature.

3. Results and discussion

3.1. Structural and morphological characterization

The XRD patterns of $LiNi_{0.5}Mn_{1.5}O_4$ powders synthesized under different holding times are illustrated in Fig. 1. All prepared samples present XRD patterns of cubic $LiNi_{0.5}Mn_{1.5}O_4$ spinels with typical intensive peaks, such as (1 1 1), (3 1 1), (4 0 0) and (4 4 0). Peaks corresponding to NiO appear at the side shoulders of (3 1 1) and (4 0 0), which are clearly labeled in the middle section of Fig. 1. More intensive impurity peaks in the samples A and D are observed compared with the other two samples, and the insufficient calcination time is the reason for sample A. The right section of Fig. 1 is the enlarged profile of the (4 4 0) peak. This peak of the samples A and C shifts towards higher and lower angle, respectively, compared with the peak position in the samples B and D. The lower shift indicates an increase in lattice parameter [23], therefore the sample C has the largest lattice framework and the sample A is smallest. For confirming the conjecture, cell parameters of all samples were calculated and tabulated in Table 1. The volume of samples, which is similar with the previous reports [24,25], increases gradually and reaches the maximum value of 0.5453 nm^3 for sample C, then decreases with increasing the holding time. The results from Table 1 are well consistent with the above inference. We note that the oxygen release from the lattice is inevasible during the high temperature calcining process, which induces the decline of the total negative valence. The lower oxidized state of Mn^{3+} having larger ionic radius

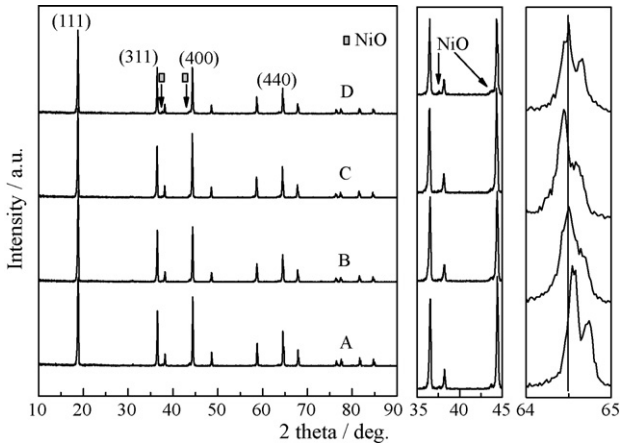

Fig. 1. XRD patterns of $LiNi_{0.5}Mn_{1.5}O_4$ powders prepared for 6 h (A), 12 h (B), 18 h (C) and 24 h (D), the enlarged profile of peak (3 1 1) and (4 0 0) for the middle part, the enlarged profile of peak (4 4 0) for the right part.

than that of corresponding cation, Mn^{4+}, is introduced due to neutral charge compensation. The lattice volume largely depends on the amount of Mn^{3+} in the compound $LiNi_{0.5}Mn_{1.5}O_4$ spinels [26]. As shown in Fig. 1 and Table 1, the lattice volume increases with the holding time up to 18 h, suggesting that the Mn^{3+} content is reduced afterwards. Thus, partial Mn^{3+} ions should been oxidized back to Mn^{4+} by oxidant O_2 due to Mn^{3+} ions can be suppressed by the oxygen partial pressure [27]. Since all samples were fabricated under similar conditions except for holding times, and more NiO impurity existed in sample D compared with the sample C, therefore we presume that a prolonged time could impel the spinel to decompose accompanied with oxygen release. The decomposition products may include Li_2MnO_3 and NiO which are both detected in the final powder prepared at an extreme synthesis condition [11]. However, the investigation is uncompleted for the absent compound with Mn^{3+}. In order to thoroughly understand this phenomenon, a rigorous calcining condition was adopted on the spinel precursor identically prepared as above samples. The sample was obtained by being sintered at 900 °C for 18 h and the XRD pattern is shown in Fig. 2. It is worth noting that a new impurity peak corresponding to Mn_2O_3 located at the left shoulder of the peak (3 1 1) appears. Therefore, the spinel is unstable under the rigorous situation and decomposes as shown in the following equation which is different from Eq. (1).

$$4LiNi_{0.5}Mn_{1.5}O_4 \rightarrow 2Li_2MnO_3 + 2Mn_2O_3 + 2NiO + O_2 \quad (2)$$

The oxygen released by this side reaction can oxidize partial Mn^{3+} into Mn^{4+}, thus reducing the lattice volume for sample D (see Table 1 and Fig. 1). Based on above results, powders sintered for 12 h and 18 h (samples B and C) have good crystallinity verified by the sharp peaks and high purity.

*Fd*3*m* and $P4_332$ two different space groups belong to $LiNi_{0.5}Mn_{1.5}O_4$ spinel and are distinguished with each other by the Ni ordering in the lattice. A better electrochemical performance can be expected for the spinel with *Fd*3*m* space group compared with the other group due to a 2.5 orders of magnitude faster elec-

Table 1
Lattice parameters of the $LiNi_{0.5}Mn_{1.5}O_4$ synthesized for 6 h (A), 12 h (B), 18 h (C) and 24 h (D).

Samples	Lattice parameter/nm	Volume/nm^3
A	0.8157	0.5423
B	0.8162	0.5437
C	0.8171	0.5453
D	0.8164	0.5441

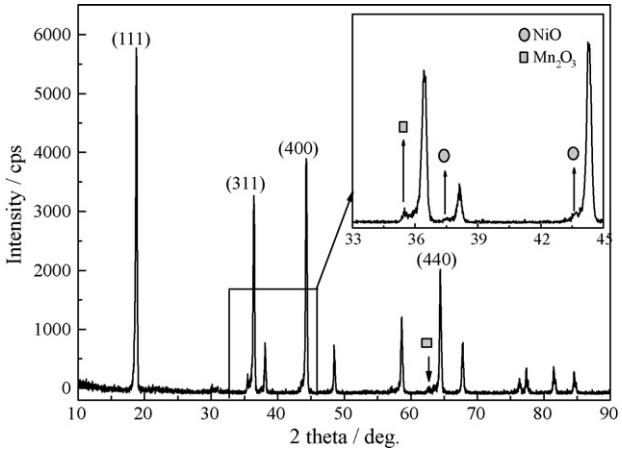

Fig. 2. XRD patterns of $LiNi_{0.5}Mn_{1.5}O_4$ powders prepared at 900 °C for 18 h.

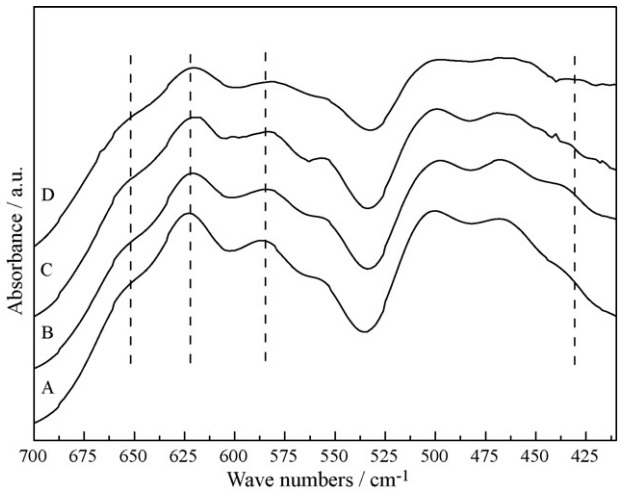

Fig. 3. FTIR spectra of $LiNi_{0.5}Mn_{1.5}O_4$ powders prepared for 6 h (A), 12 h (B), 18 h (C) and 24 h (D).

tronic conductivity [28]. However, the space difference is difficult to determine with XRD technique owing to a similar scattering behavior of Ni and Mn. As a useful tool, the FTIR spectroscopy is applied to identify the cation ordering in this work [29]. The FTIR spectra in the range from 700 cm^{-1} to 420 cm^{-1} of the spinels sintered for different times are presented in Fig. 3. More intensive band at 623 cm^{-1} compared to that at 587 cm^{-1}, as illustrated in Fig. 3, is a typical feature of the *Fd*3*m* space group [28]. The absent or undefined bands at 650 cm^{-1} and 428 cm^{-1} in the FTIR spectra, which is a feature of the $P4_332$ space group, further demonstrate the as-fabricated samples being the *Fd*3*m* space group. It is noted that sample D has a stronger band at 428 cm^{-1} compared with other materials (samples A–C), which suggests an announced alleviated cation disordering degree. It is reported that the spinel with an ordered cation arrangement can be obtained by heat treatment under an oxygen rich atmosphere [30]. Therefore, for sample D, partial disordered mixing cations are regulated by the oxygen released from the decomposition reaction, which further confirms the decomposition occurrence.

Surface morphology and particle size distribution are both important factors affecting the electrochemical performances of

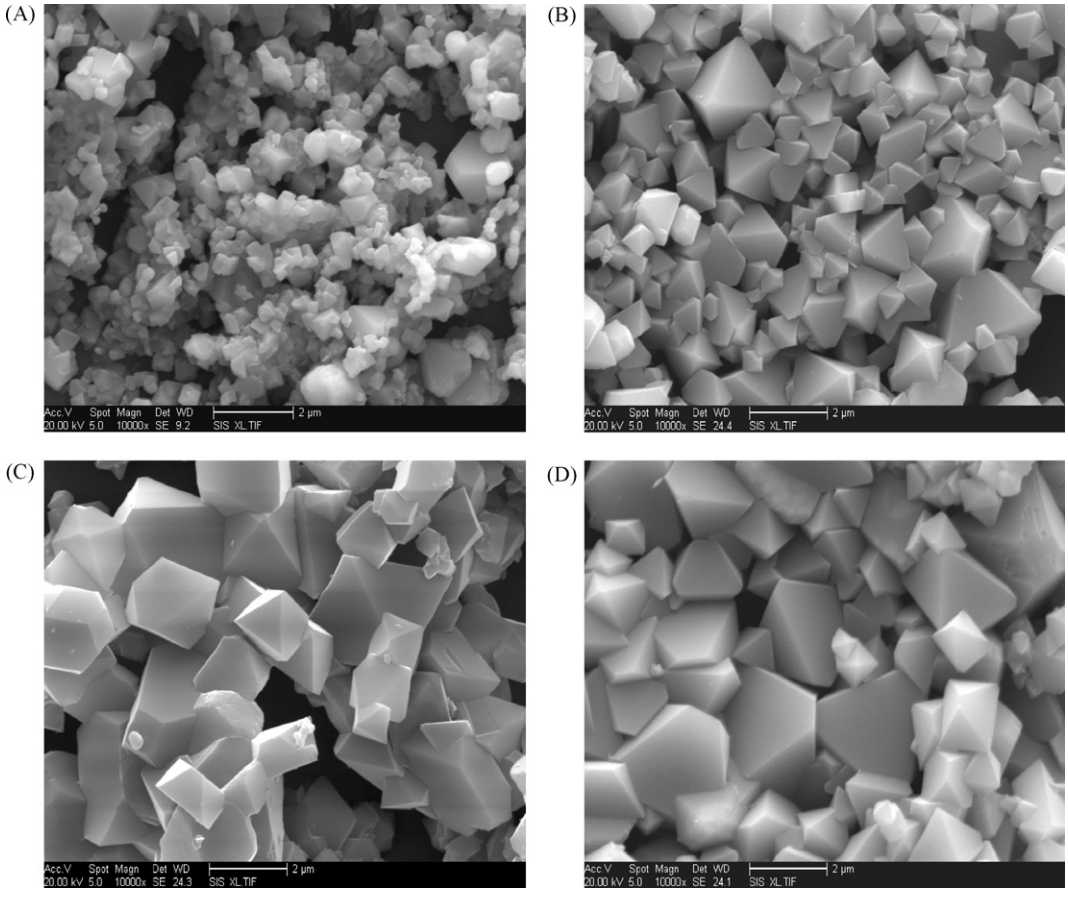

Fig. 4. SEM images of the $LiNi_{0.5}Mn_{1.5}O_4$ synthesized for 6 h (A), 12 h (B), 18 h (C) and 24 h (D).

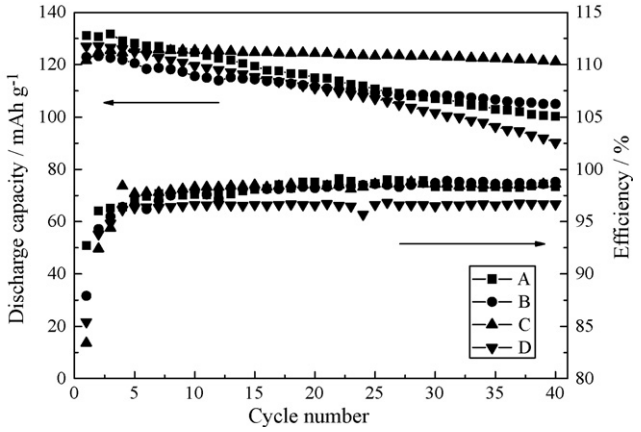

Fig. 5. Cycling performance and efficiency curves of the $LiNi_{0.5}Mn_{1.5}O_4$ synthesized for 6 h (A), 12 h (B), 18 h (C) and 24 h (D).

electrode materials, so particle size and morphology of all samples synthesized for 6 h, 12 h, 18 h and 24 h were examined by SEM. As shown in Fig. 4, the holding time plays a significant role on the appearance development of powders. The particle presents better defined polyhedral faces, which describes a high crystallinity, larger grain size, and narrower particle size distribution with prolonging the holding time. Sample A presents the smallest average particle size, undeveloped morphology and the broadest particle size distribution. Few observed polyhedral particles indicate that crystallization is in progress, which is well consistent with the analysis in XRD. An improving morphology is observed in sample B, nevertheless the particle size distribution is broad. By contrast the samples C and D possess smooth polyhedral morphology, nevertheless despite the particle size distribution in sample D becomes decrescent, a more homogeneity is observed in sample C. The electrochemical performances are strongly affected by the morphology, the particle size distribution, and the purity, combined with the analysis from XRD, the sample C should have the best electrochemical behaviors.

3.2. Electrochemical characterization

The cycling performance of the as-prepared samples is shown in Fig. 5. The cell was charged and discharged at 0.2 C rate over the voltage range from 3.0 V to 4.95 V. Clearly, the holding time has an important role on the electrochemical behavior. Among all tested samples, the sample C has a stable cycling performance. The capacities after 40 cycles account for 76.46%, 85.38%, 99.70% and 70.98% of the initial valves of cathodes for samples A–D, respectively. The abrupt capacity decay for sample A can mainly be explained by the larger surface area due to the small particle size, the more impurity phase arising from the insufficient calcining time and the wider particle size distribution, for sample B mainly being the wide grain size distribution, and for sample D being the deterioration caused by decomposition impurity phases, respectively.

The efficiency curves of the spinels prepared with various holding times are also shown in Fig. 5. Clearly, all samples present a flat efficiency curve after activation for the first 5 cycles. Similar to the cycling performance, the sample C presents a better efficiency. In light of the results from XRD and SEM measurements, the better cycling performance of sample C could be attributed to its good crystallinity, narrow particle size distribution and big particle size with small surface area where less decomposition side reaction with the electrolyte occurs.

The rate performance of cathode active materials with high voltage plateau is needed for high power capability of mobile power

Table 2
Rate capacity of the $LiNi_{0.5}Mn_{1.5}O_4$ spinels prepared for 6 h (A), 12 h (B), 18 h (C) and 24 h (D).

Rate/C	Capacity/mAh g^{-1}			
	A	B	C	D
0.2	130.22	122.50	125.47	128.06
0.5	129.09	119.09	124.74	128.32
1	122.50	121.14	124.98	127.55
3	108.18	111.57	121.75	122.45
5	97.27	99.46	115.69	115.31

sources. The discharge capacities at different rates (from 0.2 C to 5 C rate) between 3.0 V and 4.95 V (versus Li/Li$^+$) are summarized in Table 2. The cell was charged with 0.2 C rate to 4.95 V before the discharge test. As shown in Table 2, the capacity of spinels generally decreases when increasing the discharge current from 0.2 C to 5 C. The discharge capacity decreases slightly for all tested samples when the discharge current is less than 1 C, and only for these samples calcined for 18 h and 24 h (samples C and D) as the discharge current goes up to 3 C and 5 C. In order to verify the rate capability of various samples, capacities have been normalized to 100% capacity for the value measured at the rate of 0.2 C. The retentions of different samples as a function of discharge rate are presented in Fig. 6. We can conclude that the samples made with longer holding time have improved retentions, especially the high rates at 3 C and 5 C. It is well documented that the reduced particle size benefits the high rate performance due to a shorter lithium ion diffusion length. In our study, the material synthesized for 6 h (sample A) having the smallest grain size among all compounds (indicated by SEM image in Fig. 4) should have a superior rate capability. But this expectation is contradicted to our experimental results (see Fig. 6). We ascribe the result to the different Mn^{3+} ion contents in the final product, which is related to the holding time, since all materials were synthesized under similar conditions. The kinetics of Li intercalation (de-intercalation) into (from) the spinels' lattice can be improved by weakening the repulsion force between lithium ions and transition metal ions in the host structure, for example lowering the oxidation state of metals ions. Therefore, the best rate capability in sample C can be explained by the highest concentration of Mn^{3+} ions among all tested samples, illustrated by XRD and the lattice parameter measurements, as well as the high crystallinity which is important for lithium ion diffusion in the spinel structure.

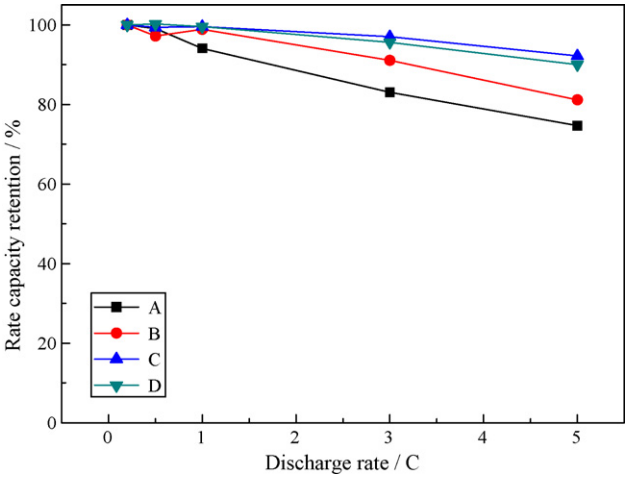

Fig. 6. Rate capacity retentions of the $LiNi_{0.5}Mn_{1.5}O_4$ synthesized for 6 h (A), 12 h (B), 18 h (C) and 24 h (D).

4. Conclusions

In this study, spinel $LiNi_{0.5}Mn_{1.5}O_4$ cathode materials were successfully synthesized with sol–gel method. The performance of $LiNi_{0.5}Mn_{1.5}O_4$ cathode for lithium ion battery is strongly depended on holding times. The experimental results show that the Mn^{3+} amount in the compound increases with prolonging the holding time till to 18 h, which introduces an improvement in rate behavior. Whereas, the self-decomposition deteriorating the material's cycling performance occurs when further increasing the holding time (24 h), and the rate capability is worsened due to larger repulsion force between lithium ions and transition metal ions arising form the partial oxidization of Mn^{3+} to Mn^{4+} by the product of the released oxygen. An appropriate longer holding time (18 h) improves the spinel's polyhedral morphology, the crystallinity, the particle size distribution, thus, the stable cycling performance. A high rate capacities being 121.75 mAh g^{-1} and 115.69 mAh g^{-1} at the discharge rate of 3 C and 5 C, accounting for 97% and 92% of the initial capacity measured at 0.2 C rate, respectively, and a capacity retention of 99.7% after 40 cycles are obtained for the compound calcined at 850 °C for 18 h. We further remark that such composition with high voltage, stable cycling and good rate performances is a promising positive candidate for lithium ion battery in high power applications.

References

[1] D.K. Kim, P. Muralidharan, H.W. Lee, R. Ruffo, Y. Yang, C.K. Chan, H.L. Peng, R.A. Huggins, Y. Cui, Nano Lett. 8 (2008) 3948–3952.
[2] Y.S. Lee, Y.K. Sun, S. Ota, T. Miyashita, M. Yoshio, Electrochem. Commun. 4 (2002) 989–994.
[3] G. Derrien, J. Hassoun, S. Panero, B. Scrosati, Adv. Mater. 19 (2007) 2336–2340.
[4] G.Q. Liu, Y.J. Wang, Qilu, W. Li, Chenhui, Electrochim. Acta 50 (2005) 1965–1968.
[5] X.X. Xu, J. Yang, Y.Q. Wang, Y.N. NuLi, J.L. Wang, J. Power Sources 174 (2007) 1113–1116.
[6] T. Ohzuku, S. Takeda, M. Iwanaga, J. Power Sources 81–82 (1999) 90–94.
[7] T.A. Arunkumar, A. Manthiram, Electrochim. Acta 50 (2005) 5568–5572.
[8] M. Okada, Y.S. Lee, M. Yoshio, J. Power Sources 90 (2000) 196–200.
[9] Q.M. Zhong, A. Bonakdarpour, M.J. Zhang, Y. Gao, J.R. Dahn, J. Electrochem. Soc. 144 (1997) 205–213.
[10] B. Markovsky, Y. Talyossef, G. Salitra, D. Aurbach, H.J. Kim, S. Choi, Electrochem. Commun. 6 (2004) 821–826.
[11] J.H. Kim, S.T. Myung, Y.K. Sun, Electrochim. Acta 49 (2004) 219–227.
[12] Y.K. Sun, K.J. Hong, J. Prakash, K. Amine, Electrochem. Commun. 4 (2002) 344–348.
[13] B.J. Hwang, Y.W. Wu, M. Venkateswarlu, M.Y. Cheng, R. Santhanam, J. Power Sources 193 (2009) 828–833.
[14] Y. Idemoto, I. Narai, N. Koura, J. Power Sources 119–121 (2003) 125–129.
[15] H. Fang, Z. Wang, X.H. Li, H.J. Guo, W.J. Peng, J. Power Sources 153 (2006) 174–176.
[16] S.T. Myung, S. Komaba, N. Kumagai, H. Yashiro, H.T. Chung, T.H. Cho, Electrochim. Acta 47 (2002) 2543–2549.
[17] Y.K. Fan, J.M. Wang, X.B. Ye, J.Q. Zhang, Mater. Chem. Phys. 103 (2007) 19–23.
[18] L.J. Fu, H. Liu, C. Li, Y.P. Wu, E. Rahm, R. Holze, H.Q. Wu, Prog. Mater. Sci. 50 (2005) 881–928.
[19] Z.Q. Liu, W.L. Wang, X.M. Liu, M.C. Wu, D. Li, Z. Zeng, J. Solid State Chem. 177 (2004) 1585–1591.
[20] Y.K. Fan, J.M. Wang, Z. Tang, W.C. He, J.Q. Zhang, Electrochim. Acta 52 (2007) 3870–3875.
[21] G.D. Du, Y.N. NuLi, J. Yang, J.L. Wang, Mater. Res. Bull. 43 (2008) 3607–3613.
[22] T.F. Yi, J. Shu, Y.R. Zhu, R.S. Zhu, J. Phys. Chem. Solids 70 (2009) 153–158.
[23] M. Aklalouch, R.M. Rojas, J.M. Rojo, I. Saadoune, J.M. Amarilla, Electrochim. Acta 54 (2009) 7542–7550.
[24] R. Alcántara, M. Jaraba, P. Lavela, J.L. Tirado, Electrochim. Acta 47 (2002) 1829–1835.
[25] K. Ariyoshi, S. Yamamoto, T. Ohzuku, J. Power Sources 119–121 (2003) 959–963.
[26] L.F. Xiao, Y.Q. Zhao, Y.Y. Yang, X.P. Ai, H.X. Yang, Y.L. Cao, J. Solid State Electrochem. 12 (2008) 687–691.
[27] S.H. Oh, S.H. Jeon, W.I. Cho, C.S. Kim, B.W. Cho, J. Alloys Compd. 452 (2008) 389–396.
[28] M. Kunduraci, J.F. Al-Sharab, G.G. Amatucci, Chem. Mater. 18 (2006) 3585–3592.
[29] R. Alcántara, M. Jaraba, P. Lavela, J.L. Tirado, Chem. Mater. 16 (2004) 1573–1579.
[30] J.H. Kim, S.T. Myung, C.S. Yoon, S.G. Kang, Y.K. Sun, Chem. Mater. 16 (2004) 906–914.